XVIII IMEKO WORLD CONGRESS
Metrology for a Sustainable Development
September, 17 – 22, 2006, Rio de Janeiro, Brazil

ITERATIVE MODEL-BASED IMAGE RECONSTRUCTION FOR ULTRASOUND PROCESS TOMOGRAPHY

Gerald Steiner [1], *Frank Podd* [2], *Markus Brandner* [1], *Daniel Watzenig* [1]
[1] Institute of Electrical Measurements and Measurement Signal Processing,
Graz University of Technology, Graz, Austria, gerald.steiner@ieee.org
[2] Tomography Ltd., Leeds, UK, frank@tomography.ltd.uk

Abstract: Ultrasound process tomography is a method for imaging the acoustic impedance or sound velocity distribution within a closed pipe or vessel. It can be used for the determination of process parameters, like flow rates and material fractions, in industrial multi-phase flows. Many approaches are based on reflection measurements and the assumption of piece-wise constant acoustic impedance distributions. For this configuration we present a novel iterative approach for image reconstruction. Reflecting objects, like gas bubbles, are modeled by B-spline contours. The inverse problem of determining the object position and shape from the reflection measurements at the boundary of the vessel is solved using a quasi-Newton optimization algorithm. The forward problem, i.e. the simulation of the measurement given the object parameters, is solved using an efficient formulation based on Fermat's principle. The model-based approach offers the advantage of always yielding closed contours. Both reflection and transmission measurement data can be used in a unified manner. The feasibility of the approach is demonstrated using simulated data.

Keywords: flow imaging, image reconstruction, process tomography, ultrasound tomography.

1. INTRODUCTION

Process tomography is concerned with imaging multi-phase material distributions in industrial environments. It can be used to determine process parameters like flow rates and material fractions. One measurement principle that has been investigated in this context is based on ultrasonic waves. Ultrasonic wave propagation is sensitive to changes in acoustic impedance, acoustic velocity, and attenuation. Depending on the used signal processing methods the spatial distribution of one of these parameters can be imaged. The approaches reported in the literature are mostly based on sensing the acoustic impedance distribution in discrete two-phase flows through reflection or transmission measurements of ultrasonic waves (see e.g. [1-5]). Many industrial processes offer very high contrast in terms of acoustic impedance, e.g. gas-liquid and gas-solid flows. At gas-liquid and gas-solid interfaces virtually all of the acoustic energy is reflected back due to the very small impdance of gases compared to liquids and solids, resulting in a very high acoustic impedance mismatch.

A typical setup for ultrasound process tomography in the cross-section of a pipe comprises a transducer array evenly distributed around the pipe circumference. The transducers can act as both transmitters and receivers. For one projection measurement one transducer is excited with a broadband pulse to transmit a pulse wave into the flow medium. The transducers are designed to emit a beam that is fan-shaped within the measurement plane and collimated in the axial direction. All transducers then act as receivers to collect parts of the emitted wave that have been directly transmitted across the pipe or reflected at material interfaces. The desired information is contained in the travel times of the received pulses. The acquired data forms a single projection. Several projections need to be collected by using different transducers as transmitters. An image showing the locations of reflecting boundaries is finally reconstructed using the totality of acquired data.

A common method for reconstructing images from the projection measurements is backprojection [1-3,6]. It is a pixel-based approach that basically consists of summing up the contributions of single measurements to the pixel values in the measurent plane. In transmission tomography only directly transmitted pulses are used and backprojected onto straight lines connecting the transmitting and receiving transducer. In reflection tomography, which is also the basis of our approach, the backprojections take the form of nonlinear curves. A pulse transmitted and received by the same transducer gives rise to a circular arc centered at the transducer location. If transmitter and receiver are different the backprojection is an ellipsoidal arc with the focii of the ellipse at the transducer position. The images obtained from backprojection suffer from heavy blurring and artifacts due to the large arc fractions that do not correspond to the physical material interfaces. A large number of ultrasonic transducers is necessary to obtain a good spatial resolution. The reconstructed images can be improved by using a filtered backprojection algorithm [6]. However, the background noise level is increased, especially for configurations with a limited number of transducers.

In typical situations both reflected and through-transmitted pulses are detected by the receivers. Transmitted pulses can be incorporated by subtracting the backprojection from the image matrix [3,4]. However, degradations may occur where object contours are located very close to

through-transmission paths. Then the transmission backprojection may reduce the pixel value of boundary pixels [7].

A threshold filter is often applied to the reconstructed images. The thresholded image contains only two kinds of pixels: interface pixels corresponding to material boundaries, and background pixels corresponding to bulk of either material. In an ideal situation the interface pixels would give a closed contour and allow the unambiguous calculation of the material fractions. However, the reconstructed contours are not closed in many cases and noise pixels present in the image additionally complicate the image interpretation. Isolated noise pixels can be removed with image processing filters to enhance the result.

An approach to derive closed contours from the thresholded backprojection image was presented in [8]. It is based on the Hough transform which is able to identify patterns from incomplete and noisy images. It maps objects in cartesian coordinates to a parameter space, where a single point corresponds to the parameter set defining a certain instance of the object. It is able to treat multiple objects without further modfications. However, the computational complexity is exponentially increasing with the number of parameters since the dimension of the parameter space increases accordingly. So only circles of variable radius have been considered in the mentioned approach.

A direct model-based approach to image reconstruction was applied in [5], where the position and diameter of the air core of a hydrocyclone was measured for varying configurations of the device. Tailored to this specific application, the air core was approximated by a circle. The diameter and the position of the circle were fitted to the reflection data using a simplified model assuming small deviations from the central position.

In this work we present a general model-based approach to image reconstruction. Material inclusions in the background medium are modeled by closed curves. These are parameterized B-spline functions, allowing for a wide range of possible shapes beyond circles. The model parameters are identified using a quasi-Newton optimization algorithm. To allow for real-time image reconstruction using this iterative algorithm an efficient simulation of the measurement problem is required, which is described in the subsequent section.

2. FORWARD PROBLEM

A crucial component of iterative reconstruction algorithms for real-time process tomography applications is the efficient solution of the forward problem. In our case it consists of simulating the measured pulse arrival times for a given material distribution in the measurement plane. Since it has to be solved multiple times, usually once in every iteration, it has a major impact on the execution time of the algorithm.

The sensor configuration used as basis of our measurement is illustrated in Fig. 1, where 16 transducers are evenly spaced around the pipe circumference. The transducers emit a wide fan-shaped beam in the cross-section of the pipe defining the measurement plane, as sketched by the dashed lines. It should be collimated and very thin in axial direction. The measurement plane in the example contains a

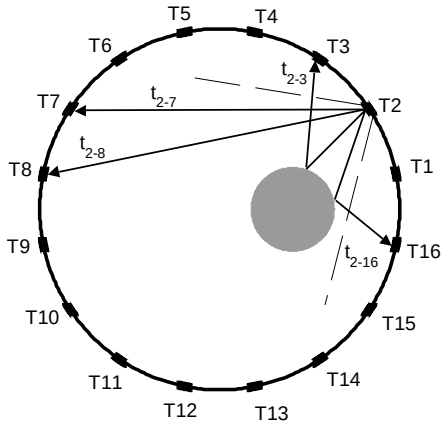

Fig. 1. Typical sensor configuration for ultrasound reflection tomography. The pipe defining the measurement plane holds 16 transducers T1 – T16. The transducers have a fan-shaped beam in the imaging plane. Different pulse travel times for reflected and transmitted pulses are recorded as different transducers are used as transmitters.

circular material inclusion. The received signals depend on the position and shape of the inclusion. We take discrete gas-liquid or gas-solid flows as basis of our approach and assume perfect reflection of the ultrasonic waves at material interfaces. This simplification can be made due to the striking difference in acoustic impedance. The pressure reflection coefficient of an acoustic plane wave incident on the interface between a propagation medium with impedance Z_1 and a medium with impedance Z_2 is:

$$R_p = \frac{Z_2 - Z_1}{Z_1 + Z_2} \tag{1}$$

At a water-air interface, e.g., the reflection coefficient is 99.8% [9]. A further assumption is that the ratio of the object dimensions to the acoustic wavelength in the background medium is large so that specular reflection can be assumed and diffraction effects are negligible.

Fig. 1 indicates some of the recorded pulse travel times for the case of T2 acting as transmitter. Direct through-transmissions are, e.g., detected by T7 and T8. The transmissions can be distinguished from reflected pulses because their travel times are known from the fixed geometry of the setup if the sound velocity in the background medium is known. T3 to T6 are outside of the beam region of T2, so that no direct transmission occurs with these. The emitted wave is partially reflected at material interfaces and can, e.g., be detected by T3 and T16.

A possibility to simulate the forward problem of ultrasound reflection tomography under the mentioned assumptions is ray-casting [10]. The sound beam emitted by a transducer is finely discretized in rays, resembling geometrical optics. Every ray is followed from the source until an intersection with a reflecting obstacle or the pipe occurs. The reflected ray is determined using the law of reflection and further propagated. Rays that hit receiver positions are recorded. This approach is able to cope with arbitrary obstacle configurations and can account for multiple reflections. However, the simulation is rather costly due to the need for fine discretization in order to obtain reliable results.

To allow for fast image reconstruction with iterative algorithms a different approach based on Fermat's principle is

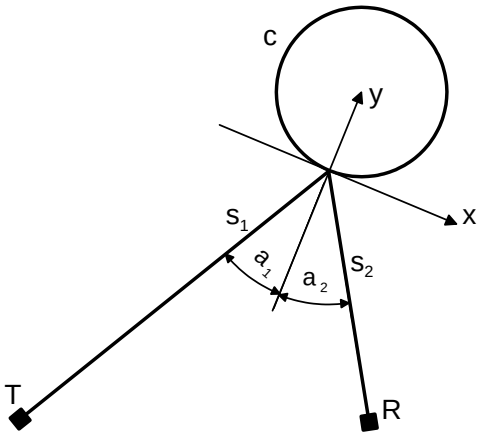

Fig. 2. Reflection of an acoustic ray emitted from transmitter T, reflected at the contour c, and incident on the receiver R.

proposed, stating that the acoustic path length between two transducers must be minimal. An acoustic ray reflected at an arbitrary contour c on its way from the transmitter T to the receiver R is sketched in Fig. 2. Without loss of generality a local Cartesian coordinate system (x, y) is assumed, with the axes parallel to the surface tangent and normal at the point (x_C, y_C) under consideration on the contour c. The total travel time of the ray is determined by the sound velocity v_L and the transmitter, reflection point, and receiver coordinates with subscripts T, C, and R, respectively:

$$t_t = \frac{1}{v_L}(s_1 + s_2) = \frac{1}{v_L}\left(\sqrt{(x_C - x_T)^2 + (y_C - y_T)^2} + \ldots \right. \\ \left. \ldots\sqrt{(x_R - x_C)^2 + (y_R - y_C)^2}\right) \quad (2)$$

The partial derivative of the travel time with respect to a displacement of the reflection point along the contour is:

$$\frac{\partial t_t}{\partial x_C} = \frac{1}{v_L}\left(\frac{x_C - x_T}{s_1} - \frac{x_R - x_C}{s_2}\right) = \frac{1}{v_L}(\sin a_1 - \sin a_2) \quad (3)$$

A necessary condition for a minimum of the travel time of a ray reflected at (x_C, y_C) is that (3) equals zero. Since the involved angles are always smaller than $\pi/2$ this is only satisfied if $a_1 = a_2$ in agreement with the law of reflection.

This offers a convenient way to determine the travel time of single-time reflected pulses. The reflecting contour is discretized and the path lengths are calculated for all points on the contour. The desired path length is the minimal value under the constraint that there are no intersections of the path with a reflecting contour. This simulation of the forward problem can be easily solved for arbitrary reflectors since only simple algebraic operations and a minimum search are necessary. Multiple reflections are not considered in our case because this would exponentially increase the required number of investigated ray paths. If such multiple reflections occurred in the measurement they would lead to a remaining residual in the solution of the inverse problem. They are also a nuisance in backprojection reconstruction since they can not be resolved and lead to wrong backprojections.

3. PARAMETERIZED B-SPLINE CONTOURS

As outlined in the previous section the boundaries between gas and liquid phases are described by means of a contour c in 2D. In a general formulation the contour is given by a vector-valued function $\Re \to \Re \times \Re : s \to c(s)$ where the parameter $s \in [0,1]$ indicates the position of a given point on the contour. c is closed if and only if *c(0)=c(1)*. The B-spline contour model represents each point *c(s)* as a linear combination of constant basis functions weighted by a set of N control points [13]. In the practical implementation the control points are arranged into a *(2N x 1)* state vector *q*. The number of parameters required to fully parameterize the shape can be reduced by introducing the shape space representation of B-splines as outlined in Eqn. (4). The shape space is given by a linear transformation that maps a shape space vector (i.e. the state vector) to a spline vector *q* using a reference spline q_0.

$$q = Wx + q_0 \quad (4)$$

Compared to the dimension of the spline vector the low dimensional state vector allows for a considerable reduction in the complexity of the shape representation. The reference contour can be freely chosen, offering the flexibility to incorporate various levels of prior knowledge. The shape matrix *W* enforces that deviations from the reference spline are bound to geometrically meaningful deformations. We apply the five degrees of freedom affine transformation that allows for translations, rotation, scaling, and shear of 2D splines. Fig. 3 depicts a reference spline (dashed contour) and five instances that are derived by applying a Gaussianly distributed random state vector to the shape space representation of the spline.

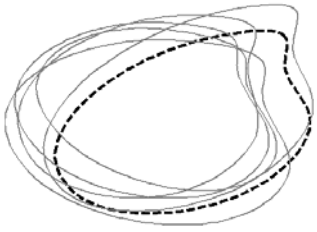

Fig. 3. Reference spline represented by the black dashed contour and five random instances depicted in gray.

4. INVERSE PROBLEM

For our model-based approach the inverse problem consists of finding the parameter vector x^* that best fits the available measurement data. For the present study we restrict ourselves to single inclusions, so that there are 6 unknowns in the inverse problem. We solve it by minimizing the cost functional $J(x)$, which is composed of the sum of squared errors of the measured and simulated ultrasonic pulse travel times weighted with the measured peak amplitudes u_i:

$$x^* = \arg\min_x J(x) = \sum_{i=1}^{n} u_i (t_{i,meas} - t_{i,sim}(x))^2 \qquad (5)$$

One issue when evaluating the cost functional is the number of measurements n in the summation. When r transducers are used the maximum is $n = r^2$ when every transducer acts as transmitter and all transducers receive a signal. However, in real situations the beam angle of the transmitting transducer is finite, so that only some of the receivers will detect a through-transmitted signal in an empty pipe. If a reflecting inclusion is present in the imaging plane some of the transmission paths may be blocked in addition. This occurrence depends on the positions and shapes of material inclusions. For the summation in (5) we only use finite travel times, i.e. recorded signals without an incoming pulse in both measurement and simulation are excluded. So n is redetermined at every iteration of the reconstruction algorithm. The single travel time errors are weighted with the measured peak amplitude of the respective pulses. Low amplitude pulses are less reliable than high amplitude pulses because the relative impact of noise and unwanted coupling and wave propagation effects is higher. Therefore they are assigned a lower impact on the total value of the cost functional.

To solve (5) we use a quasi-Newton algorithm with BFGS update for the Hessian approximation [11]. A cubic polynomial line search method is used for the steplength determination. The gradient of (5) is calculated through finite differencing since no direct gradient information can be obtained from the numerical solution of the forward problem. The optimization algorithm is terminated if the improvement in the cost functional is below a predefined threshold.

5. RESULTS

An ellipsoidal gas inclusion in water imaged by 16 transducers in circular aperture configuration is used as simulation example to validate the proposed reconstruction approach. The synthetic measurement data was generated with a ray-casting algorithm. The algorithm incorporates characteristics of physical measurement systems like impulse responses, thresholding circuits, beam profiles of the transducers, and measurement. The gas inclusion was placed in the upper right part of the pipe.

The reconstruction result using the standard backprojection algorithm is shown in Fig. 4. The contour of the ellipse can be recognized, but there is considerable blurring and background noise from the backprojected arcs. The sensitivity of ultrasound process tomography is highest in the center of the imaging region and rather low close to the pipe wall. There are even blind spots very close to the pipe between the single transducers due to the finite beam angle. The inhomogeneous sensitivity distribution can be clearly seen in the image. The backprojected images are often thresholded to remove the artifacts, although it may be hard to choose the optimal threshold value. The sensitivity distribution can be partially compensated for by nonlinear thresholding [12].

The reconstruction of the gas inclusion using the proposed iterative model-based approach is illustrated in Fig. 5, where the evolution of the contour over the iterations are shown. A circular reference shape was employed and used as initial contour at the center of the pipe, as indicated by iteration number 0. The further progression of the algorithm is shown with the thin contours and the corresponding iteration numbers. The final result, obtained after 10 iterations, is the thick black contour. The gray dashed ellipse shows the true object position and shape. It is well matched by the econstructed contour, avoiding the problems associated with backprojection reconstructions. The course of the cost functional value over the iterations is depicted in Fig. 6, showing the well-posed behavior of th reconstruction process for the example.

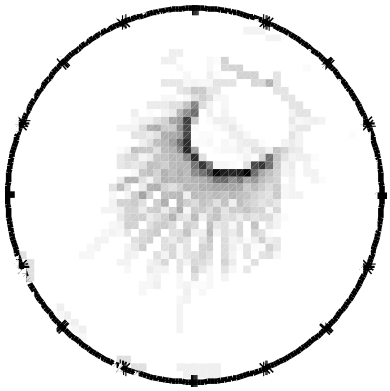

Fig. 4. Reconstruction result for an ellipsoidal gas bubble in water obtained with the backprojection algorithm. The considerable blurring and inhomogeneous sensitivity distribution degrade the image quality.

The same test distribution was used to analyze the convergence region for the inverse problem. The algorithm was initialized with the same reference contour as in Fig. 5, but at different positions. The obtained cost functional values as function of the center of the initial circular contour is shown in Fig. 7. The center of the true inclusion is indicated by the black dot. Function values below 100 correspond to a good fit between true and reconstructed contour. For the case

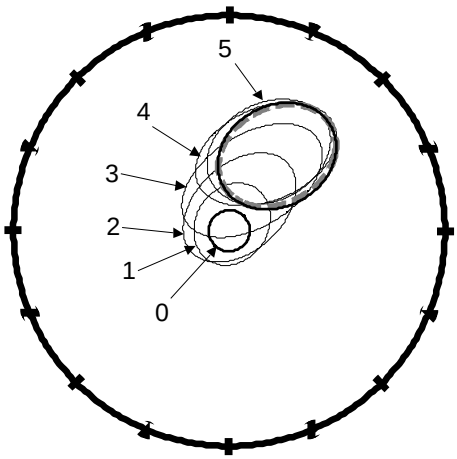

Fig. 5. Reconstruction result with the B-spline-based nonlinear least squares approach. The gray dashed ellipse shows the true bubble location. The thin black curves show the evolution of the contour at the indicated iteration numbers, and the thick black curve is the obtained solution.

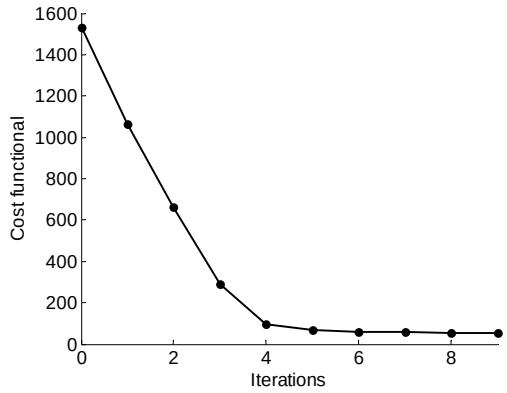

Fig.6. Evolution of the cost functional value during the Gauss-Newton iterations for the shown example. The minimization process is terminated after 10 iterations.

shown in Fig. 5, e.g., the final value is $J = 52$. Values of 100 and above indicate divergence of the algorithm to a local minimum, with a final object location far from the true position. It can be seen that the stability range includes the full quadrant containing the true inclusion and conveniently extends beyond the center of the pipe. So an initial position at the center of the pipe seems to be sufficient to achieve convergence even for rather remotely located true shapes.

6. CONCLUSION

Ultrasound reflection tomography can be used as a tool to monitor industrial multi-phase processes. We consider the case of two-phase gas-liquid or liguid-solid material distributions, which offer significant contrast in terms of acoustic impedance. Image reconstruction in the cross-section of the process vessel is commonly performed using backprojection algorithms. The results usually suffer from blurring, artifacts and noise pixels, although the situation can be partly improved using advanced image processing methods.

One property of the pixel-based backprojection reconstruction is that it cannot be guaranteed that the contours of material inclusions, which are effectively imaged, are closed. This issue motivated the introduction of a novel approach to reconstruction that ensures closed contours and inherently avoids the occurrence of artifacts. We use a model of material inclusions formulated as closed contours based on B-splines and try to match the parameter vector to the true contour by solving a least squares problem. A special formulation of the forward problem ultilizing Fermat's principle that allows an efficient numerical simulation of the measurement is introduced, enabling the application of iterative optimization algorithms.

The performance of the algorithm is demonstrated by a simulation study based on ray-casting, yielding appealing results. Future work will have to further investigate the behavior of the proposed approach on a broader basis and under varying conditions with physical measurement data. In addition, the detection of multiple independent material inclusions will be addressed.

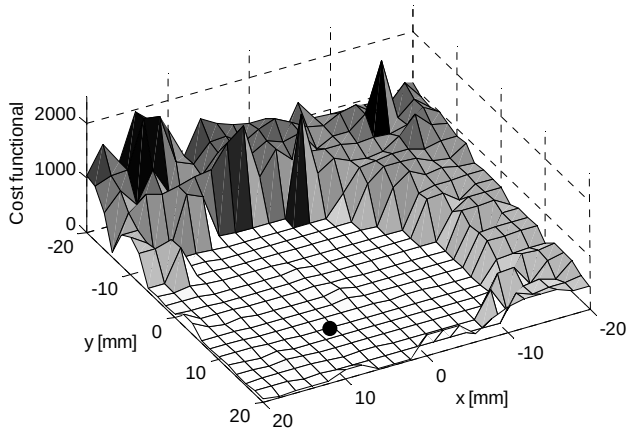

Fig. 7. Cost functional values as a function of the initial contour position for the shown example. The algorithm converges within a convenient radius around the center of the pipe.

REFERENCES

[1] L.J. Xu and L.A. Xu, "Ultrasound Tomography System Used for Monitoring Bubbly Gas/Liquid Two-Phase Flow", IEEE Trans. on Ultrasonics, Ferroelectrics and Frequency Control, Vol. 44, No. 1 , pp. 67-76, January 1997.

[2] H.I. Schlaberg, F.J.W. Podd, and B.S. Hoyle, "Ultrasound Process Tomography System for Hydrocyclones", Ultrasonics, Vol. 38, pp. 813-816, 2000.

[3] M. Yang, H. I. Schlaberg, B. S. Hoyle, M. S. Beck and C. Lenn, "Real-Time Ultrasound Process Tomography for Two-Phase Flow Imaging Using a Reduced Number of Transducers", IEEE Transactions on Ultrasonics, Ferroelectrics and Frequency Control, Vol. 46, No. 3, pp. 492-501, May 1999.

[4] W. Li and B.S. Hoyle, "Ultrasonic Process Tomography Using Multiple Active Sensors for Maximum Real-Time Performance", Chemical Engineering Science, Vol. 52, No. 13, pp. 2161-2170, 1997.

[5] F. Podd, H. I. Schlaberg and B. S. Hoyle "Model-Based Parameterisation of a Hydrocyclone Air-Core", Ultrasonics, Vol. 38, pp. 804-808, 2000.

[6] M. Moshfeghi, "Ultrasound Reflection-Mode Tomography Using Fan-Shaped-Beam Insonification", IEEE Transactions on Ultrasonics, Ferroelectrics and Frequency Control, Vol. UFFC-33, No. 3, pp. 299-314, May 1986.

[7] A. Plaskowski, M.S. Beck, R. Thorn, and T. Dyakowski, "Imaging Industrial Flows: Applications of Electrical Process Tomography", Institute of Physics Publishing, 1995.

[8] M. Yang, H.I. Schlaberg, B.S. Hoyle, M.S. Beck, and C. Lenn, "Parallel Implemented Hough Transform for Pattern Recognition in Ultrasound Process Tomography", Proceedings of Frontiers in Industrial Process Tomography, pp. 349-356, Delft, The Netherlands, April 1997.

[9] G.S. Kino, "Acoustic Waves: Devices, Imaging and Analog Signal Processing", Prentice Hall, 1987.

[10] F. Wiegand and B.S. Hoyle, "Simulations for Parallel

Processing of Ultrasound Reflection-Mode Tomography with Applications to Two-Phase Flow Measurement", IEEE Transactions on Ultrasonics, Ferroelectrics and Frequency Control, Vol. 36, No. 6, pp. 652-660, November 1989.

[11] R. Fletcher, "Practical Methods of Optimization", John Wiley & Sons, 1987.

[12] D.T. Pham, M. Yang, and Z. Wang, "Non-Linear Adaptive Threshold for Ultrasound Image Process", Proceedings of the 7th International Conference on Signal Processing (ICSP), Vol. 2, , pp. 975 - 977, Beijing, China, September 2004.

[13] A. Blake and M. Isard, "Active Contours", Springer, 1998.